Applied Chemical Engineering (2022) Volume 5 Issue 2
doi:10.24294/ace.v5i2.1638

ORIGINAL RESEARCH ARTICLE

Application of an experimental design in the hydrothermal synthesis of GIS-NaP zeolite from brickwall wastes

Marcelo Rodríguez Valdivia*, Rivalino Guzmán Ale, Martha Huamán Gutiérrez

Escuela Profesional de Ingeniería de Materiales, Facultad de Ingeniería de Procesos FIP, Universidad Nacional San Agustín de Arequipa, Arequipa, Peru. E-mail: materiales@unsa.edu.pe

ABSTRACT

This article reports the results of an investigation carried out in order to obtain zeolitic material of the GIS-NaP type with high cation exchange capacity using brick waste. The hydrothermal synthesis was carried out in a stainless-steel reactor using NaOH activating solutions at concentrations of 2.0, 2.5 and 3.0 M, activation temperatures of 100, 120 and 140 °C and activation times of 7, 8 and 9 hours. The product obtained was characterized by X-ray Fluorescence, Scanning Electron Microscopy (SEM), X-ray Diffraction, and Cation Exchange Capacity (CEC).

The results obtained showed that for the hydrothermal conversion test at 140 °C/2 M/7 hours, GIS-NaP synthetic zeolite with a cation exchange capacity equal to 163.5 meq/100 g was obtained. The statistical analysis, applying a factorial experimental design, indicated that the main factors with a great effect on the cation exchange capacity (CEC) are the activation temperature and the interaction between it and the concentration of the activating solution, with a degree of significance of 0.049250 and 0.056631 for a confidence level of 90.82%. An empirical mathematical model was developed and validated by applying ANOVA analysis that considers the interaction effects of all factors and was optimized by applying the response surface methodology.

Keywords: Brick Waste; Cation Exchange Capacity; GIS-Nap Zeolite; Factorial Experimental Design; Hydrothermal Synthesis

ARTICLE INFO

Received: 12 April 2022
Accepted: 20 June 2022
Available online: 11 July 2022

1. Introduction

Worldwide, the construction industry represents a very important economic activity in the development of each country. In addition to consuming thousands of tons of non-renewable natural resources, it generates large amounts of waste, the disposal of which has an impact on the environment[1].

Among these wastes are bricks made of clay, which represent a large and rapidly increasing volume due to the great need for housing by the population[2]. In order to comply with environmental regulations, many researches and publications have raised its management and reuse as aggregates for concretes, geotextiles, soil stabilization, flexible pavements, etc.,[3,4], so as to reduce the amount of waste that is transferred to landfills[5].

Zeolites are microporous materials consisting of tetrahedral crystalline structures of alumina (AlO_4) and silica (SiO_4) that give rise to a three-dimensional lattice bonded by oxygen atoms[6]. They are widely used for pollution control due to their high performance and low production cost[7]. Synthetic NaP zeolite with GISmondine structure type (GIS) possesses high cation exchange capacity and due to its small pore

size is widely used in gas separation, removal of heavy metals, ammonium, radioactive elements, seawater treatment, water softening, water softener in detergent industry[8,9].

The hydrothermal synthesis process (hydrothermal treatment) consists of three stages: dissolution, condensation and crystallization. The process of transformation of a mineral precursor into zeolite could be represented as follows[10,11]:

$$(SiO_2 + 3Al_2O_3{\cdot}2SiO_2 + \text{aluminosilicates, glassy matrix} + NaOH \text{ solution (80–180 °C)} \longrightarrow$$
$$\underset{(Mineral\ precursor)}{}$$
$$\underset{(Mixture\ reaction)}{SiO_4^{4-} + Al_2O_4^{5-} + Na^+ + OH^-} \longrightarrow \underset{(Zeolite)}{Na_{x/n}[Al_xSi_yO_{2(x+y)}]{\cdot}zH_2O}$$

Where x (between 2 to 10), z, y (between 2 to 7); are integers corresponding to the unit cell. Na is a metal cation with valence n = 1.

Several authors define that the variables or factors to be considered to obtain zeolites via hydrothermal conversion are temperature, reaction time and NaOH concentration and that the application of an experimental design allows to better analyze the effect of these factors on a response and seeks the optimization of the synthesis process[12].

In the present research work, the synthesis of GIS-NaP zeolite using brick waste from building demolition is proposed due to its high SiO_2 and Al_2O_3 contents[13], which allow the application of a successful hydrothermal treatment. It is also sought to statistically evaluate the effect of the conversion factors on the cation exchange capacity.

In the first stage, the brick residue is characterized by chemical and physical analysis. For the conversion process, NaOH solutions at different concentrations with different temperatures and treatment times are used. In a second stage, the zeolitic product obtained is characterized by chemical analysis with X-ray fluorescence, morphological analysis with electron microscopy (SEM), crystal identification with X-ray diffraction and determination of the cation exchange capacity (CEC). The study of the effect of the factors is performed by applying a two-level factorial experimental design with STATISTIC V.5 software.

2. Experimental

2.1 Materials and methods

(1) Material. It is made up of pieces of brick from the demolition of buildings in the city of Arequipa-Peru. On a sample of 5 kg, granulometric analysis was performed in order to determine the distribution of particle size classes. Fine material of 100 microns was used for the experimental tests.

(2) Characterization and analysis equipment. The chemical composition was determined using an X-ray fluorescence spectrometer (XRF) S4 Explorer manufactured by Bruker AXS. Morphological analysis of the brick residue and zeolitic product was carried out using a FEI Quanta 200 high and low vacuum electron microscope (SEM) with SED and BSED microanalysis detectors. The identification of zeolitic crystals was performed using a Rigaku miniflex II X-ray diffractometer**,** with a CuKα (1.5405 Å) radiation source, with a step of 2θ = 0.002º and a time per step of 10 seconds. Data were collected over a range of 0 to 60° 2Θ. For the evaluation of cation exchange capacity (CEC), double cation exchange tests were performed using 1.0 N sodium acetate and 1.0 N ammonium acetate solutions. Na^+ exchange analysis was performed using a Perkin Elmer OPTIMA-2100-DV ICP adsorption equipment at Laboratorios del Sur.

(3) Reagents. The solutions used were prepared with the following salts: NaOH (99.5%), $NaC_2H_3O_2{\cdot}3H_2O$, $NH_4C_2H_3O_2{\cdot}3H_2O$ (99.0%), isopropyl alcohol (99.0%), purchased from Diproquim.

(4) GIS-NaP zeolite production. The tests to obtain synthetic zeolite were carried out using an AISI 304 stainless steel vessel that was placed inside an oven at temperatures of 100, 120 and 140 ℃. These parameters are close to those used by Wang, *et al.*[14], who report having obtained NaP zeolite using activation temperatures between 80 and 120 ℃ from met. In the container, 10 g of brick residues and NaOH solutions with M concentrations were placed, maintaining a solid/liquid ratio of 12.5. The

activation time (contact between the liquid) was 7, 8 and 9 hours. The product obtained was washed with distilled water and filtered and finally dried in an oven at 60 ºC for 6 hours, conditions defined according to the reviewed literature[15].

(5) Cation exchange capacity (CEC). The analytical method of double cation exchange using sodium acetate and ammonium acetate solutions was employed[16]. The cation exchange capacity is determined on the basis of the Na^+ content exchanged and expressed in meq/100 g.

(6) Two-level factorial experimental design. In order to evaluate the effect of the experimental conditions on the hydrothermal conversion process of the brick waste, a two-level factorial experimental design was used. This design is very consistent and allows defining the optimum conditions of the process through the analysis of variance. STATISTIC V.5 software was used for this purpose. Three independent factors were evaluated: activation temperature, NaOH activating solution concentration, activation time. The dependent response was the cation exchange capacity. **Table 1** describes the factors and levels evaluated.

Table 1. Factors and levels of the factorial design

Factors	Level (-)	Level (+)
Activation temperature (°C)	100	140
Activating solution (M)	2	3
Activation time (hours)	7	9

3. Results and discussions

3.1 Characterization of brick waste

(1) Chemical composition. Table 2 presents the analysis of brick residue in its natural state according to the literature[3].

The ground brick residue has a SiO_2 + Al_2O_3 content equal to 89.38%. According to the literature consulted[17], they indicate that this ratio should be approximately 89%, and that these constitute a determining factor in the type of zeolite to be formed. Compounds containing Ca, Fe are impurities that can limit the application of this precursor in the synthesis of zeolites. It presents main mineralogical constituents corresponding to quartz, feldspar and hematite[18].

Table 2. Chemical composition-residue of brick[3]

Compounds	Na_2O	MgO	Al_2O_3	SiO_2	K_2O	CaO	Fe_2O_3	TiO_2	H_2O	LOI
Measure	%	%	%	%	%	%	%	%	%	%
	0.20	0.04	25.49	63.89	0.95	0.29	7.73	0.00	1.33	0.95

LOI: Loss on ignition determined by gravimetry.

(2) Morphological characterization

Figure 1 shows regular shaped particles of different size with high content of fine material.

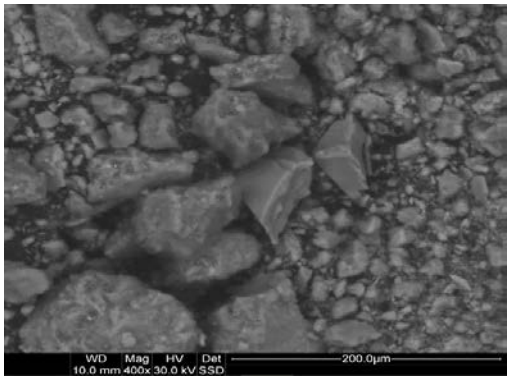

Figure 1. SEM scanning micrograph showing ground brick particles.

(3) Cation exchange capacity (CEC). **Table 3** presents the cation exchange capacity (CEC) determined on samples of the zeolitic products obtained at different test conditions and for the untreated material.

Figure 2 presents the ionic interca capacity as a function of the weight loss ratio Pf/Pi (Pf = final weight, Pi = initial weight) which is n the efficiency of the hydrothermal synthesis process[19].

In the 140 °C/2 M/7 hours condition, the weight loss ratio (Pf/Pi) is 0.859 with respect to the other tests performed and corresponds to the highest cation exchange capacity (163.48 meq/100 g). For the 100 °C/3 M/7 hours condition there is a ratio of 0.856 but a cation exchange capacity of (129.57 meq/100 g.). The weight loss is related to the lower or higher dissolution of silica and alumina, which finally affects the degree of crystallization of the zeolite. According to Szeremen *et al.*[20], the cation exchange capacity depends on the anionic charge density (Al^{3+} and Si^{4+} substitution) of the formed

zeolite structure. For the particular case, the low cation exchange capacity is due to the low crystallinity of GIS-NaP zeolite formed by partial transformation of the amorphous phase (SiO_2) at 100 °C[21].

Table 3. Cation exchange capacity (CEC)

Test	Test Conditions	(CEC) meq/100g
1	100 °C/2 M/7 h	107.39
2	140 °C/2 M/7 h	163.48
3	100 °C/3 M/7 h	129.57
4	140 °C/3 M/7 h	97.83
5	100 °C/2 M/9 h	88.70
6	140 °C/2 M/9 h	129.57
7	100 °C/3 M/9 h	87.39
8	140 °C/3 M/9 h	109.57
9	120 °C/2.5 M/8 h	127.39
10	120 °C/2.5 M/8 h	110.87
11	120 °C/2.5 M/8 h	133.04
12	Ground brick	2.10

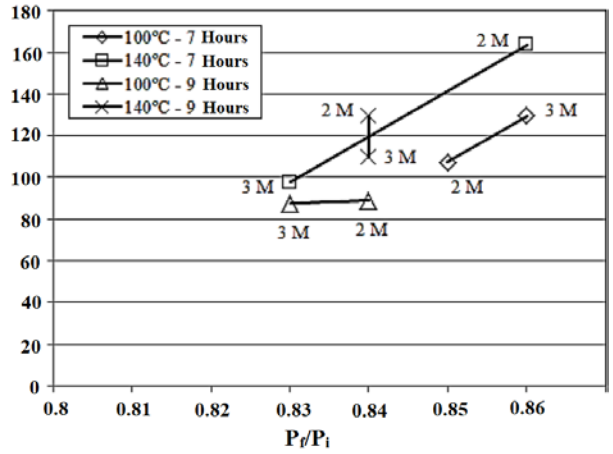

Figure 2. Cation exchange capacity as a function of weight loss.

(4) Chemical composition of GIS-NaP zeolite. On the synthetic zeolite that presented the highest cation exchange capacity (140 °C/2 M/7 hours), a chemical and morphological characterization was performed in order to identify the type of synthetic zeolite formed. **Table 4** shows the results of the chemical analysis expressed in oxides present.

(5) Morphological characterization. Figure 3 shows pseudospherical crystal formations of GIS-NaP zeolite. These results are similar to those presented by Hildebrando *et al.*[22], who claim to have identified GIS-NaP zeolite with pseudospherical morphology in the hydrothermal synthesis of metakaolin at 100 °C and 20 hours of treatment. Authors such as Ali *et al.*[23], call pseudospherical formations as aggregates of crystals with cactus/cactus morphology. They obs formations are constituted by small plates with well-defined edges indicating an otal.

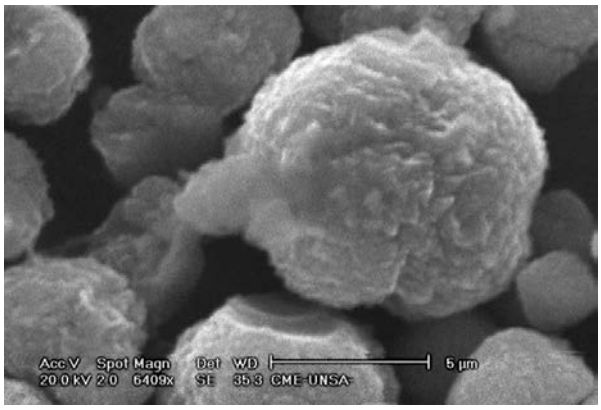

Figure 3. Formation of pseudospherical crystals of GIS-NaP zeolite. Test 140 °C/2 M/7 h.

(6) X-Ray Diffraction. Hong *et al.*[24] claim to have obtained peaks of high intensity at 12.5º, 17.6º, 21.6º, 28.2º, and 33.4º, which are clear characteristics of NaP zeolite formation. Coincidentally, the diffract obtained in this study shows main peaks at 12.4º, 17.62º, 21.56º, 28.04º and 33.34º; which confirms that it is a NaP zeolite of type GIS.

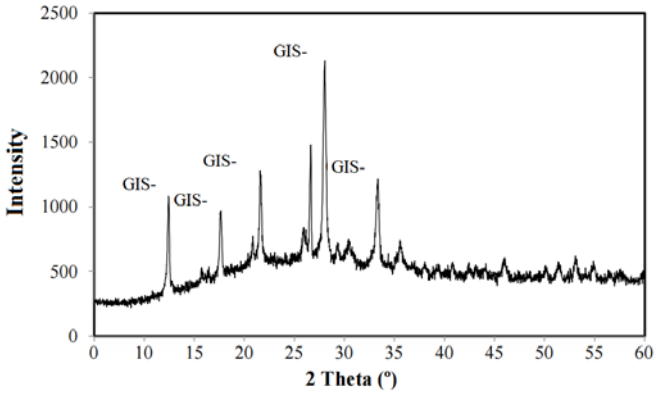

Figure 4. X-ray diffraction of GIS-NaP zeolite.

(7) Statistical analysis ANOVA. Table 5 presents the results of the analysis of variance (ANOVA) for the factorial model considering the effect of each factor (i), (ii), (iii); as well as the effect caused by their interactions 1*2, 1*3, 2*3, 1*2*3. The result of the ANOVA analysis for the factorial model considers the sum of squares of the treatments (SS), the degrees of freedom (df), the sum of squares of the means (MS). The evaluation of the incidence of treatment effects was performed by using the F distribution. The p-value statistic allows comparison

with the significance value $\alpha = 0.10$[25,26]. If $p < \alpha$, the null hypothesis is rejected and it is concluded that the corresponding effect is active or influences the response variable. The quantity R-sqr = 0.90818, indicates that CEC values with approximately 90.82% variability are obtained, while Adj. (R-sqr adj.) equal to 0.69394; corresponds to the size-adjusted value or the number of factors in the model.

Table 4. Chemical composition - synthetic zeolite

Compounds	**Na_2O**	**Al_2O_3**	**SiO_2**	**K_2O**	**MgO**	**CaO**	**Fe_2O_3**	**Mn_2O_3**	**LOI**
Measure	%	%	%	%	%	%	%	%	%
	6.96	26.81	54.24	5.64	0.60	0.11	2.05	0.13	3.34

LOI: Loss on ignition determined by gravimetry.

Table 5. Analysis of variance for the factorial model

Factor	**SS**	**df**	**MS**	**Fo**	**p**
(1) Activation temperature	954.845	1	954.845	6.151667	0.089250
(2) Solution concentration	524.556	1	524.556	3.379495	0.163307
(3) Activation time	861.955	1	861.955	5.553217	0.099713
1*2	1,418.314	1	1418.314	9.137602	0.056631
1*3	187.211	1	187.211	1.206124	0.352342
2*3	61.383	1	61.383	0.395466	0.574063
1*2*3	597.542	1	597.542	3.849716	0.144560
Error	465.652	3	155.217		
Total SS	5,071.459	10			

ANOVA; Var. CEC; R-sqr = 0.90818; Adj: 0.69394; 2** (3-0) desing: MS Residual = 155.2173 DV: CEC

From the Fo analysis, it can be seen that the most significant effect is the interaction between activation temperature and activating solution concentration, followed by activation temperature and activation time. The p values (0.056631, 0.089250 and 0.099713) are less than $\alpha = 0.10$; therefore, they influence the cation exchange capacity (CEC).

(8) Analysis of the main effects and their interactions. The interaction of the three conversion factors on the CEC can be best represented in a Pareto diagram[26]. **Figure 5** presents the Pareto diagram for the effects of the factors (TEMPACTI = Temperature of activation, TIEMPACT = Time of activation and CONCSOLU = Concentration of activating solution).

Figures 6, **7** and **8** show the individual effects for the factors TEMPACTI = Temperature of activation, TIEMPACT = Time of activation and CONCSOLU = Concentration of activating solution).

As can be seen in **Figures 4**, **5**, **6** and **7**, the activation temperature has a positive effect on the cation exchange capacity. On the contrary, the activation temperature and the concentration of the activating solution have a negative effect. The CEC temperature measurement and its adjustment is fundamental in the experimental process.

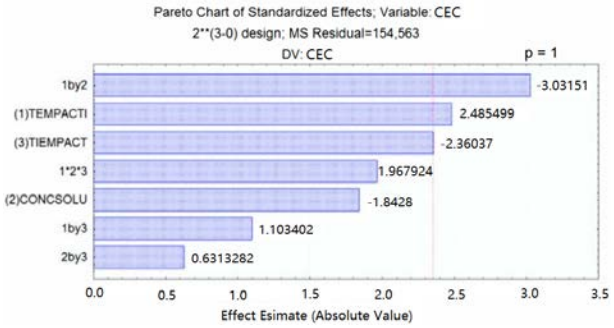

Figure 5. Pareto branch diagram for factors.

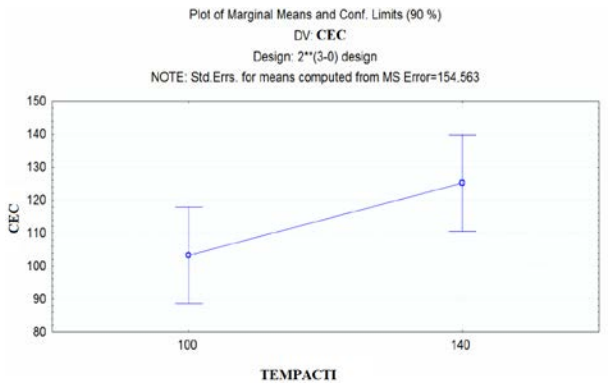

Figure 6. Effect of activation temperature on the Cation Exchange Capacity (CEC).

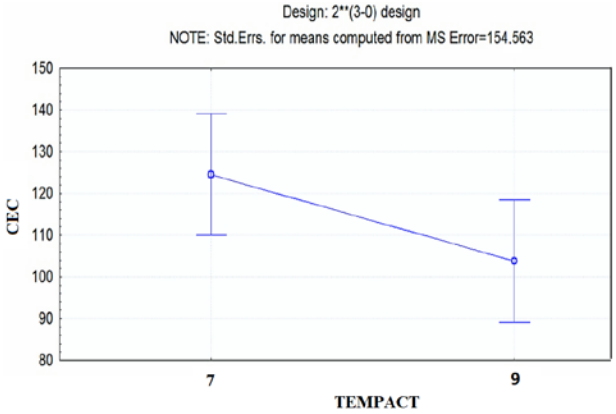

Figure 7. Effect of activation time on Cation Exchange Capacity (CEC).

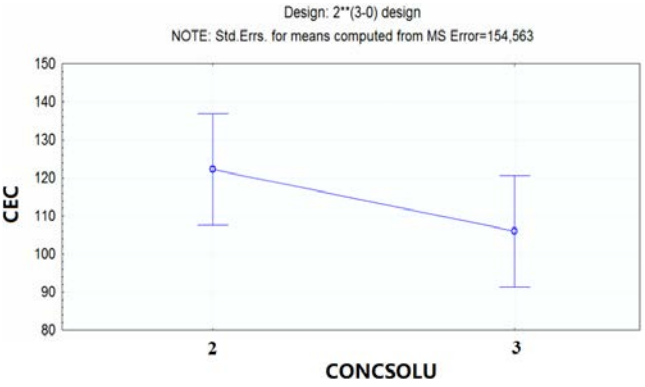

Figure 8. Effect of the concentration of the activating solution on the Cation Exchange Capacity (CEC).

Figures 9, **10** and **11** present the effect of the interactions between the factors TEMPACTI = Temperature of activation and CONCSOLU = Concentration of activating solution,

It is clearly evident that there is a strong inverse interaction between the activation temperature factors and the concentration of the activating solution (**Figure 7**), which cause reaching high values of cation exchange capacity CEC. Using a temperature of 140 °C, the CEC turns out to be increased in important quantities with a concentration of activating solution of 2 M NaOH. There is a significant interaction between activation time and temperature, and activating solution concentration and activation time (**Figures 8** and **9**) as the lines between the actual values are not completely parallel. With an activation time of 7 hours, the CEC is improved when tested at an activation temperature of 140 °C. The magnitude of CEC increases when using an activating solution concentration of 2 M NaOH and maintaining an activation time of 7 hours.

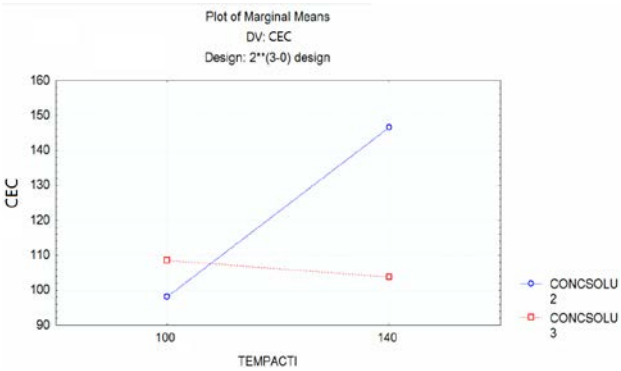

Figure 9. Effect of the interaction between activation temperature and activating solution concentration on cation exchange capacity (CEC).

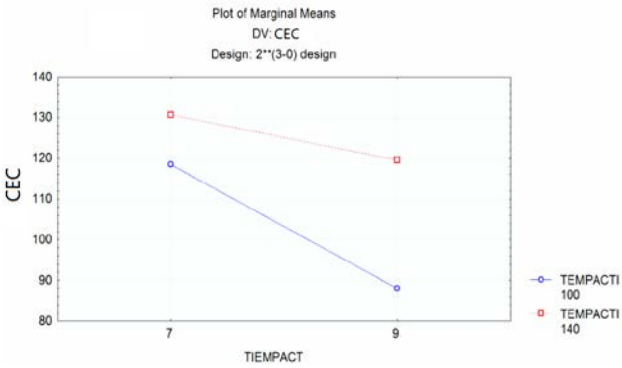

Figure 10. Effect of the interaction between activation time and activation temperature on cation exchange capacity (CEC).

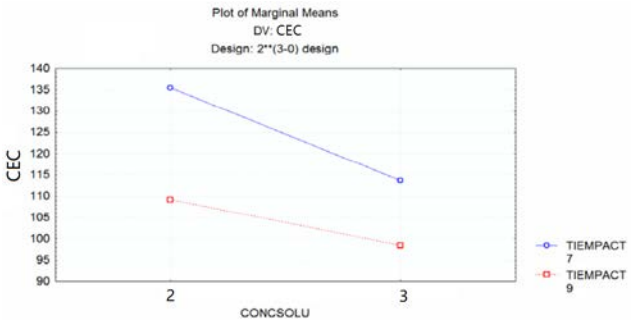

Figure 11. Effect of the interaction between the concentration of the activating solution and the activation time on the Cation Exchange Capacity (CEC).

(9) Analysis of response surface plots. Figures 12 and **13** show the three-dimensional response surface plots for the factors considered: TEMPACTI = Temperature of activation, TIEMPACT = Time of activation and CONCSOLU =Concentration of active solution.

It is well known that different combinations of variables or factors result in a high ionic capacity. The response surface between activation temperature and activating solution concentration (**Figure 11**), shows that the maximum CEC is achieved at high temperature values (140 °C) and low concentrations

(2 M). For the response surface between activation time and activating solution concentration (**Figure 12**), the best CEC is obtained at a time of 7 hours and a concentration of 2 M NaOH.

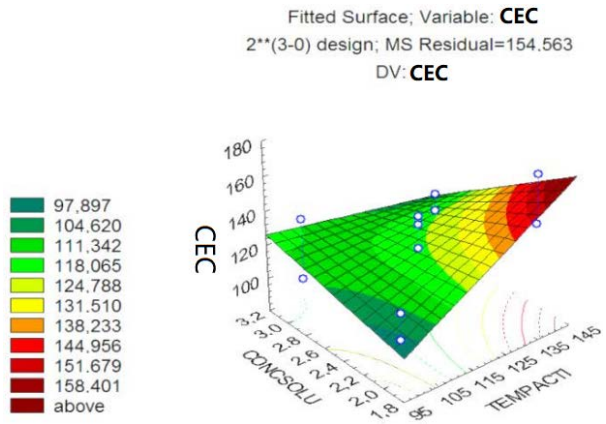

Figure 12. Surface diagram: Relationship between activation temperature and activating solution concentration on Cation Exchange Capacity (CEC).

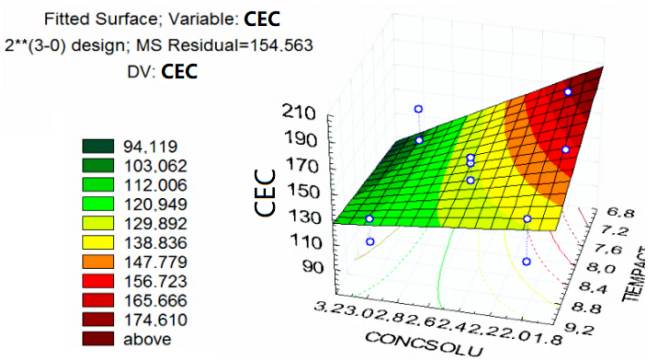

Figure 13. Surface diagram: Relationship between activation time and activating solution concentration on the Cation Exchange Capacity (CEC).

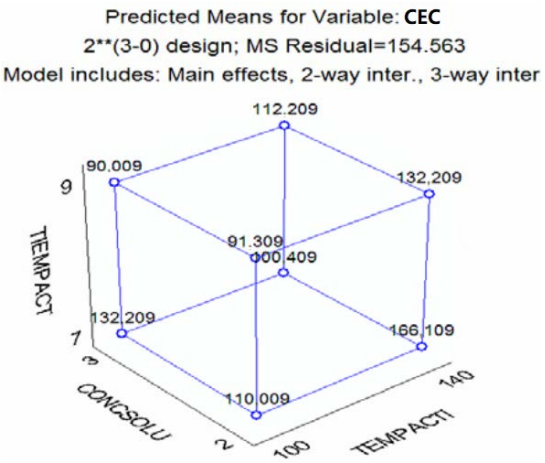

Figure 14. Cube Graph: relationship between temperature, activation time and activating solution concentration on Cation Exchange Capacity (CEC).

(10) Cube chart analysis. It is used to find the direction of improvement of the experimental process. **Figure 14**, presents the Cube plot in which the estimated response at each point of the design and how the combination of the three factors (TEMPACTI = Temperature of activation, TIEMPACT=Time of activation and CONCSOLU=Concentration of activating solution) affect the CEC. It is ue cation exchange capacity increases when the activation temperature is 140 °C, 2 M NaOH and an activation time of 7 hours.

The results obtained in the synthesis tests to obtain GIS-NaP zeolite from ground brick residue revealed that:

3.2 GIS-NaP zeolite production

(1) Effect of activation temperature. At the test condition 140 °C/2 M/7 hours, the cation exchange capacity reaches the maximum obtainable of 163.48 meq/100 g. Ji *et al.*[27] mention that at high temperatures a high zeolitic phase crystallinity is achieved due to a complete reaction between NaOH and the solid phases present in the starting material. At this temperature, a complete dissolution of Si and Al, present in the precursor, is achieved and a high formation of zeolite NaP is ensured[28,29].

(2) Effect of activating solution concentration. The highest CEC is obtained when a low concentration of the activating alkaline solution (2 M) is used. It is clearly observed that using 2 M concentrations the maximum value of CEC = 163.5 meq/100g is reached. Compared to the value shown for the brick residue CEC = 2.1 meq/100 g, there is an increase of 161.40 meq/100 g. An activating solution with a high concentration of NaOH activates the dissolution of Si and Al contained in the precursor. In addition; Na^+ promotes a high formation of soluble sodium silicate which accelerates the crystallization process of zeolite.

(3) Effect of activation time. The best results are obtained in tests with longer activation times. In particular, for times of 7 hours, the best CEC values are obtained when 2 M NaOH concentrations at 140 °C are used. This is the optimum activation time to obtain a high zeolite crystallinity. With a short time, there is no chemical reaction and the amorphous solid phase is maintained; whereas with an

excessively long time the formation of GIS-NaP zeolite crystals decreases[30].

(4) Factorial experimental design. The analysis of variance showed that the variables that directly influence the process are temperature and activation time, as well as the relationship between temperature and the concentration of activating solution with a probability of 90%. The response surface diagram allowed to identify the significance of the studied factors, their interaction and the most optimal CEC values that can be expressed in a mathematical model[31].

CEC (meq/100 gr) = −1957.19 + 19.24 (Activation temperature) + 929.70 (Activating solution concentration) + 206.15 (Activation time) − 8.25 (Activation temperature) * (Activating solution concentration) − 1.92 (Activation temperature) * (Activation time) − 98.25 (Activating solution concentration) * (Activation time) + 0.86 (Activation temperature) * (Activating solution concentration) * (Activating solution concentration) * (Activation time)

(5) Cation exchange capacity. The determination of the cation exchange capacity (CEC) showed that the highest CEC value achieved at 140 ℃/2 M/7 hours corresponds to a GIS-NaP sodium synthetic zeolite with a content of 32.7% of zeolitic crystals. Lower values would indicate the formation of zeolitic materials with low crystallization contents in GIS-NaP or formation of zeolitic crystals of different types. The CEC value is related to the crystallinity and purity of the synthesized zeolite.

4. Conclusions

Brick waste from building demolition was treated by a hydrothermal conversion process to obtain synthetic sodium zeolite of the GIS-NaP type with high cation exchange capacity (CEC).

The test carried out at 140 ℃/2 M/7 hours, allowed to obtain synthetic zeolite GIS- NaP with a cation exchange capacity equal to 163.5 meq/100 g.

The use of an experimental design proved to be a very useful tool to evaluate the different conversion conditions, determining the domains in which the factors of activation temperature, activation time and activating solution concentration can be optimized to obtain pure GIS-NaP.

The main factors with a large effect on the cation exchange capacity are the activation temperature and the interaction between the activation temperature and the concentration of the activating solution, with a significance of 0.049250 and 0.056631 for a confidence level of 90.82%.

Considering the results obtained, the use of brick waste for the production of GIS-NaP zeolite, constitutes a viable alternative and with the possibility of application for environmental remediation.

Conflict of interest

The authors declare that they have no conflict of interest.

References

1. Mobili A, Giosué CH, Corinaldesi V, *et al.* Bricks and concrete wastes as coarse and fine aggregates in sustainable mortars. Advances in Materials Science and Engineering 2018; 1–11. doi: 10.1155/2018/8676708.
2. Kadir A, Sarani N. A review of wastes recycling in fired clay bricks. International Journal of Integra Engineering 2012; 4(2): 11–24.
3. Al-Baidhani A, Al-Taie A. Review of brick waste in expansive soil stabilization and other civil engineering applications. Journal of Geotechnical Studies 2019; 4(3): 14–23.
4. Xue C, Shen A, Guo Y, *et al.* Utilization of construction waste composite powder materials as cementitious materials in small-scale prefabricated concrete. Advances in Materials Science and Engineering 2016; 1–11. doi: 10.1155/2016/8947935.
5. Zhu L, Zhu Z. Reuse of clay brick waste in mortar and concrete. Advances in Materials Science and Engineering 2020; 1–11. doi: 10.1155/2020/6326178.
6. García-Betancourt M, Ramírez S, González-Hodges A, *et al.* Low dimensional nanostructures: measurement and remediation technologies applied to trace heavy metals in water. Intech Open Science 2020; 1–24. doi: 10.5772/intechopen.93263.
7. Ren X, Qu R, Liu S, *et al.* Synthesis of zeolites from coal fly ash for the removal of harmful gaseous pollutants: A review. Aerosol and Air Quality Research 2020; 20: 1127–1144. doi: 10.4209/aaqr.2019.12.0651.
8. Behin J, Kazemian H, Rohani S. Sonochemical synthesis of zeolite NaP from clinoptilolite. Ultrasonics Sonochemistry 2015; 28(2016): 400–408. doi: 10.1016/nch.2015.08.021.
9. Sharma P, Song J, Hee M, *et al.* GIS-NaP1 zeolite microspheres as potential water adsorption material: Influence of initial silica concentration on

adsorptive and physical/topological properties. Scientific Reports 2016.
10. Sánchez-Hernádez R, López-Delgado A, Padilla I, *et al.* One-step synthesis of NaP1, SOD and ANA from hazardous aluminum solid waste. Microporous and Mesoporous Materials 2016; 226: 267–277. doi: 10.1016/j.micromeso.2016.01.037.
11. Prado PF, Nascimento M, Yokoyama L, *et al.* Use of coal ash in zeolite production and applications in manganese adsorption. American Journal of Engineering Research 2017; 6(12): 394–403. doi: 10.4136/ambi-agua.2224.
12. Khosravi H, Mirzaee M, Askari M. Modeling of pack-carburizing route by general factorial design of experiment. International Journal of Engineering Research & Technology 2014; 3(9): 947–951.
13. Robayo-Salazar R, Mejía R, Muldorf-Carvajal AJ. Production of building elements based on alkali-activated red clay brick waste. Revista Facultad de Ingeniería 2016; 25(43): 21–30. doi: 10.19053/01211129.v25.n43.2016.5294.
14. Wang Y, Chen J, Wu H, *et al.* Controllable preparation of zeolite p1 from metakaolin-based geopolymers via a hydrothermal method. Clays and Clay Minerals 2017; 65(1): 42–51. doi: 10.1346/CCMN.2016.064048.
15. Utami A, Sugiarti S, Sugita P. Synthesis of NaP1 and faujasite zeolite from natural zeolite of Ende-NTT as lead (Pb(II)) adsorbent. Rasayan Journal of Chemistry 2019; 12(2): 650–658. doi: 10.31788/RJC.2019.1222056.
16. Jha B, Singh DN. A review on synthesis, characterization and industrial applications of fly ash zeolites. Journal of materials Education 2011; 33(1): 65–132. doi: 10.1002/chin.201225227.
17. Ferrarini S, Cardoso A, Paprocki A. *et al.* Integrated synthesis of zeolites using coal fly ash: Element distribution in the products, washing waters and effluent. Journal of the Brazilian Chemical Society 2016; 27(11): 2034–2045. doi: 10.5935/0103-5053.20160093.
18. Cheng H, Reuse research progress on waste clay brick. Procedia Environmental Sciences 2016; 31(2016): 218–226. doi: 10.1016/j.proenv.2016.02.029.
19. Martinez D, Cicuamia C. Synthesis and characterization of zeolites from coal fly ash (in Spanish) [Chemical Engineer Thesis]. Bogotá, Colombia: Universidad de Ciencias Aplicadas y Ambientales; 2016.
20. Szerement J, Sztanik-Kloc A, Jarosz R. Contemporary applications of natural and synthetic zeolites from fly ash in agriculture and environmental protection. Journal of Cleaner Production 2021; 311: 1–19. doi: 10.1016/j.jclepro.2021.127461.
21. Novembre D, Gimenoz D, and Del Vecchio A. Synthesis and characterization of Na-P1 (GIS) zeolite using a kaolinitic rock. Scientific Reports 2021; 11(4872): 1–11. doi: 10.1038/s41598-021-84383-7.
22. Hildebrando EA, Andrade CGB, Ferreira da Rocha CA, *et al.* Synthesis and characterization of zeolite NaP using kaolin waste as a source of silicon and aluminun. Materials Research 2014; 17(1): 174–179. doi: 10.1590/$S_1$516-14392014005000035.
23. Ali I, El-Sheikhz M, Salama T, *et al.* Controllable synthesis of NaP zeolite and its application in calcium adsorption, Science China Materials 2015; 58(8): 621–633. doi: 10.1007/s40843-015-0075-9.
24. Hong S, Um W. Top-down synthesis of NaP zeolite from natural zeolite for higher removal efficiency of Cs, Sr, and Ni. Minerals 2021; 11(252): 1–15. doi: 10.3390/min110330252.
25. Belouafa S, Chaair H, Digua K. Application of statistical experimental design and surface plot technique to optimize oxygenated apatite synthesis. Advances in Materials Science and Engineering 2020; 1–6. doi: 10.1155/2020/1034959.
26. Rahimi M, Mahmoudi J. Heavy metals removal from aqueous solution by modified natural zeolites using central composite design. Periodica Polytechnica Chemical Engineering 2020; 64(1): 106–115. doi: 10.3311/PPch.13093.
27. Da Silva Filho S, Bieseki L, Maia A, *et al.* Study on the NaOH/metakaolin ratio and crystallization time for zeolite a synthesis from kaolin using statistical design. Materials Research 2017; 20(3): 761–767. doi: 10.1590/1980-5373-MR-2015-0631.
28. Ji W, Zhang S, Zhao P, *et al.* Green synthesis method and application of NaP zeolite prepared by coal gasification coarse slag from Ningdong, China. Applied Sciences 2020; 10(2694): 1–15. doi: 10.3390/app10082694.
29. Meng X, Guo X, Zhong Y, *et al.* Synthesis of a high-quality NaP zeolite from epidesmine by a hydrothermal method. Bulletin of Materials Science 2019; 42(232): 1–8. doi: 10.1007/s12034-019-1918-x.
30. Mohammadparast F, Halladj R, Askari S. The synthesis of nano-sized ZSM-5 zeolite by dry gel conversion method and investigating the effects of experimental parameters by Taguchi experimental design. Journal of Experimental Nanoscience 2018; 13(1): 160–173. doi: 10.1080/17458080.2018.1453172.
31. Fitriyana DF, Suhaimi H, Noferi S, *et al.* Synthesis of Na-P Zeolite from geotherml sludge. Springer Proceedings 2020; 242: 51–59. doi: 10.1007/978-981-15-2294-9_5.
32. Honarmand S, Sadat Moosavi E, Karimzadeh R. Synthesis of zeolite Y from Kaolin and its model fuel desulfurization performance: Optimized by box-behnken method. Iranian Journal of Chemistry and Chemical Engineering 2020; 39(1): 79–90. doi: 10.30492/ijcce.2020.32874.